Bulgarian Chemical Communications, Volume 50, Special Issue L (pp. 102 – 112) 2018

Theoretical model for simulation of the particles drying using gateway dryer: heat and mass transfer study

A.Ghadami Jadval Ghadam*, M. Shanbehpour

Department of Chemical Engineering, Yasooj Branch, Islamic Azad University, Yasooj, Iran

Submitted March 24, 2016; Accepted August 8, 2016

In the current research, the simulation of particle drying using gateway dryer was investigated through the MATLAB software, also equations were numerically solved and the particle dehumidifying simulation process was conducted. To this aim, a theoretical model was provided which includes the unstable characteristic of both heat and mass transfer during dehumidifying the wet particle in two stages. This model provided the possibility of predicting pressure and partial dispersions of air-steam combination within the narrow pores in the shell of the wet particle. Simulation of dehumidifying process of silica particle under different conditions showed the permanent increased pressure within the narrow pores of the particle. It is pertinent to put on record that the structure of pressure and increased temperature within the core of wet particle were shown simultaneously; and also the diagrams of time changes of mass, temperature, pressure, vapor and moisture fraction were obtained.

Keywords: Simulation, Mass Transfer, Heat Transfer, MATLAB Software, Particle Drying, Gateway Dryer.

INTRODUCTION

Drying of solids is one of the oldest and most common types of operation used in different industries such as agriculture, ceramics, chemicals, food, pharmaceuticals, paper, wood, mine, polymer, and textile. This phenomenon is one of the most unknown and complicated unit operations existing; because regarding the material diversity and their behavior, there are many vague and important points that are not yet clarified [1-4]. Additionally, since modeling and its mathematical explanation must be conducted simultaneously for all three transfer phenomena including heat transfer, mass transfer and momentum (for more than one phase) and the related equations are achieved; thus it is considered as a difficult and complicated task; thus usually the drying operation is a combination of science, technology and art and the art of drying is that it is necessary to use experimental observations and process experiences in designing and choosing dryers [5]. Usually drying refers to an operation in which a liquid is separated from a solid by the use of evaporation; which means that firstly the liquid is converted to vapor and then it is easily separated; but this separation by the use of mechanical techniques such as pressing and centrifugation is not considered as drying. However, usually there is a mechanical dehumidifying stage before the drying stage; and this moisture separation by the use of mechanical operation is much easier and cheaper than the thermal methods. In some cases, instead of heat, other types of energy such as radio waves, chemical interactions etc. are used for vaporization of liquid. A liquid which is evaporated during drying is not always necessarily water; it could be volatile solvent, flammable and even toxic materials [6]. There are many types of materials that need to be dried and most of these materials have different physical and chemical properties. Also there are different methods for drying these materials and heating them. It is very difficult to categorize all drying methods. In dryers the heat is mostly transferred by application of hot air or conduction and a small part of heat is transferred through radiation. Instruments used for heat transfer through application of hot air(direct drying) or conduction, naturally provide the possibility of sending the vapor out; whereas in heat transfer through radiation where there is no need to these instruments, it is impossible to simultaneously send out the vapor; because in most cases the radiation heat transfer is not the main factor. Drying by the use of conduction is a bit different from application of hot air. In conduction, the wet solid is put into cases heated from outside and the vapor exits from the embedded hole [7, 8]. One of the most important dryers with the good performance such as reasonable accuracy, fast drying and less time is gateway dryer. Up to now only one company has conducted activities regarding gateway dryers and has introduces the first horizontal direct gateway dryer (Figure 1) [9]; but there has been no simulation operation of gateway dryer conducted up to now.

* To whom all correspondence should be sent.
E-mail: aghadami80@gmail.com; ghadami@iauyasooj.ac.ir

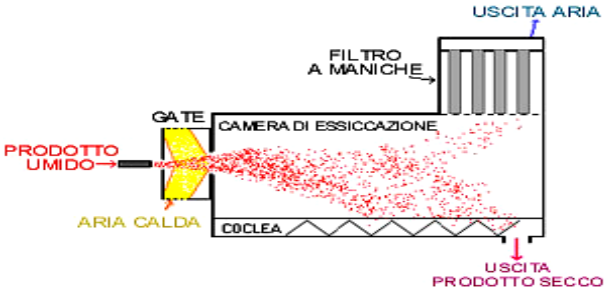

Fig. 1. Gateway dryer [9].

Typically, the drying process can be divided into two stages according to the morphology. Thus, in the first drying stage, the droplet with initial diameter ($d_{d,0}$ at Figure- 2) has greatest amount of liquid when it enters the drying medium. In the drying medium the droplet gains sensible heat (path 0–1 at Figure- 2) and then evaporation of liquid begins from the droplet surface [5]. The process of liquid evaporation results in shrinkage of the droplet diameter (path 1–2 at Figure- 2). When the amount of liquid within the droplet falls to some critical value, a very thin layer of a dry solid crust is formed at the outer surface of the droplet (point 2 at Figure- 2). From this point the second drying stage begins (path 2–3 at Figure- 2) and the droplet is treated onwards as a wet particle with constant outer diameter (d_p at Figure- 2). The wet particle includes two separated regions: solid crust, which has a porous structure, and wet core, which consists of liquid and solids. During the second drying stage, as the result of simultaneous heat transfer to the wet particle and mass transfer to the drying agent, the thickness of the solid crust continuously increases, while the diameter of the wet core (d_i at Figure- 2) shrinks. The drying stops when the amount of liquid within the particle reduces to desired value [5].

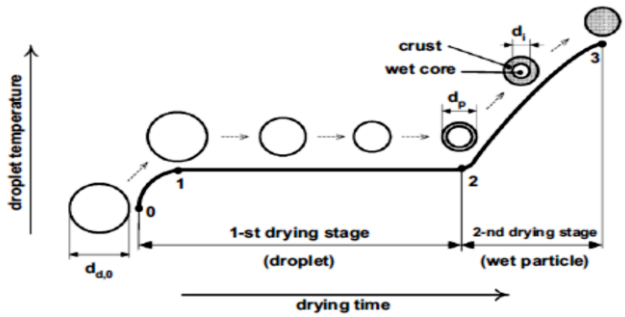

Fig. 2. Typical temperature curve and morphological changes during drying of single droplet containing solids [5].

Recently, the theoretical drying models for both types of single droplets, containing either insoluble or dissolved solids have been reviewed and published, such as a work by literature [7]. The literature survey exposed various shortcomings of published models, such as steady-state conditions for heat and mass transfer equations, ignoring initial heating-up period of droplet, unjustified neglecting wet particle temperature profile, disregarding porosity of solid crust, inaccurate calculation of mass transfer rate. Also, some of the models were neglecting crust heat absorption and simplified droplet thermo-physical properties were utilized. There was a lack of validation in a lot of cases as well [5]. Nesip Dalmaz and co-workers (2007) has provided the modeling and numerical analysis of single droplet drying which is the new developed single droplet drying model and it is used as a part of computational modeling of a typical spray dryer. This model is aimed to describe the drying behavior of a single droplet both in constant and falling rate periods using receding evaporation front approach coupled with the utilization of heat and mass transfer equations [10]. Farid (2003) has developed a model by the use of transient heat transfer equations for both wet core and dry crust regions. This model indicates this hypothesis that both internal conduction and external heat transfer resistance control the drying speed. Mass transfer resistance from the crust and also the heat effect from the diffusion of water vapor through the pores of the crust are neglected. This report has shown that drying is in the period of rate cuts and it is mainly dried and controlled by the resistance against heat transfer from the crust [11]. Cheong, et al. (1986) developed a receding interface model for the drying of sodium sulfate deca-hydrate droplets. In their study the droplets are divided to wet and dry regions separated by anevaporation interface which moves toward the center as drying proceeds. Diffusion of water vapor in the dry region is described by an effective diffusion coefficient. Both heat and mass transfer resistance of the wet region are neglected as well as sensible heating of the dry region [12]. Chen and Xie (1997) developed a model based on reaction engineering approach for the drying of milk droplets. Their model does not consider the variations of both temperature and moisture within the droplet but a proper activity coefficient is assumed to change the vapor pressure of water at the surface of the droplet. Chen et al then improved this model by introducing the crust mass transfer resistance.Although their results show good agreement with the experimental drying rates, the models fail to describe the temperature history of the milk droplets [13]. The aim of this article is simulating and investigating the parameters affecting the performance of gateway dryer in ceramic enamel production process, while the partial differential equations of heat transfer and ordinary differential equations of mass transfer have been developed for the first and second drying

stages. The period of droplet initial heating-up period, the heat capacity of the crust region, crust porosity and the temperature dependence of droplet/wet particle physical properties were also taken into account. In the second drying stage, it was assumed that the liquid evaporates from the wet core as the result of heat transfer from the drying air, and then the vapour moves through the pores of the crust towards the particle outer surface. This vapour movement inside the pores was assumed to be due to Stefan-type diffusion. From the particle outer surface the vapour was considered to be taken away by the mass convection mechanism. The corresponding mass transfer rate of the vapour was determined with the help of the steady-state equation [14]. The set of theoretical equations was numerically solved and the model was successfully validated by comparing the predicted data with corresponding experimental results, available in the literature for silica and skim milk single droplets under different drying conditions [5].

MODEL DESCRIPTION

First drying stage

In the first drying stage, drying of a motionless single droplet, containing solids, surrounded by a flow of atmospheric air, is modelled. The heat transfer in the first drying stage is considered in a general case, namely that both conditions Bi_d <0.1 and Fo_d ≥0.1 are not satisfied simultaneously. Therefore, the droplet heat capacity cannot be considered as a lumped one and a temperature profile within the droplet should be taken into account. Assuming that the droplet is a sphere with isotropic properties and the coordinate origin is at the centre of the sphere, the equation of energy conservation in spherical coordinates can be written as [7]:

$$\rho_d c_{p,d} \frac{\partial T_d}{\partial t} = \frac{1}{r^2}\frac{\partial}{\partial r}\left(k_d r^2 \frac{\partial T_d}{\partial r}\right), 0 \le r \le R_d(t) \quad (1)$$

The corresponding boundary conditions are

$$\left\{\begin{array}{ll} \frac{\partial T_d}{\partial r} = 0, & r = 0 \\ h\left(T_g - T_d\right) = k_d \frac{\partial T_d}{\partial_r} + h_{fg}\frac{\dot{m}_v}{A_d}, & r = R_d(t) \end{array}\right\} \quad (2)$$

The heat transfer from the drying air to the droplet occurs due to both convection and radiation phenomena. Therefore, the corresponding coefficient of heat transfer h can be evaluated as follows [7]:

$$h = h_c + h_r \quad (3)$$

The coefficient of convection heat transfer h_c is determined by the Nusselt number with the help of modified Ranz–Marshall correlations [15]:

$$Nu_d = \frac{d_d h_c}{k_d} = \left(2 + 0.6 Re_d^{\frac{1}{2}} pr^{1/3}\right)(1+B)^{-0.7} \quad (4)$$

where $B = c_{p,v}\left(T_g - T_d\right)/h_{fg}$ is the Spalding number. The coefficient of radiation heat transfer can be found as [16]:

$$h_r = \sigma \varepsilon_r \left(T_g^4 - T_d^4\right)/(T_g - T_d) \quad (5)$$

In the first drying stage the droplet has an excess of liquid which forms an envelope over the droplet surface, so the drying is similar to evaporation of pure liquid droplet. For this reason, the emissivity of droplet surface can be expected to be equal to this of the liquid fraction of the droplet, i.e., $\varepsilon_r = \varepsilon_{r,w}$. The rate of liquid evaporation from the droplet surface is determined as [15]:

$$\dot{m}_v = h_D\left(\rho_{v,s} - \rho_{v,\infty}\right)A_d \quad (6)$$

Here the value of mass transfer coefficient h_D is evaluated from the corresponding Sherwood number [15]:

$$Sh_d = \frac{d_d h_D}{D_v} = \left(2 + 0.6 Re_d^{\frac{1}{2}} Sc^{1/3}\right)(1+B)^{-0.7} \quad (7)$$

By assuming the elementary droplet mass decreasing is proportional to elementary droplet diameter shrinkage, the droplet shrinkage rate is found as follows [15]:

$$\frac{d(R_d)}{dt} = -\frac{1}{\rho_{d,\omega} 4\pi R_d^2}\dot{m_v} \quad (8)$$

For the droplet moisture content, X, which is defined as mass ratio of liquid and solid fractions within the droplet, the following relation can be found:

$$X = m_{d,w}/m_{d,s} = m_d\,(1 + X_{d,0})/m_{d,0} - 1 \quad (9)$$

The droplet specific heat can be evaluated according to Kirillin and Sheindlin (1956) [17]:

$$c_{p,d} = \left(\frac{\partial q_t}{\partial T}\right)_p + c_{p.w}(1-c) + c_{p,s}c \quad (10)$$

In the present study we consider only the ideal mixtures and solutions, so heat of mixing equals zero, i.e., $q_t = 0$. The mass fraction of solids and the droplet moisture content are connected:

$$c = 1/(1+X) \quad (11)$$

The droplet density can be estimated by considering a droplet as an ideal two-component mixture:

$$\rho_d = \frac{(1+X)\rho_{d,s}\rho_{d,w}}{\rho_{d,w} + X\rho_{d,s}} \quad (12)$$

In order to evaluate the droplet thermal conductivity, either series (13) or parallel (14) conceptions are applied [18]:

$$k_d = \delta k_w + (1-\delta)k_s \quad (13)$$

$$1/k_d = \delta/k_w + (1-\delta)/k_s \quad (14)$$

Where the droplet void fraction, δ, is calculated according to following expression:

$$\delta = \frac{V_{d,w}}{V_d} = 1 - 6m_{d,s}/(\pi\rho_{d,s}d_d^3) \quad (15)$$

The droplet mass can be obtained if we integrate (5):

$$m_d = m_{d,0} - 8/6\pi\rho_{d,w}(R_{d,0}^3 - R_d^3) \quad (16)$$

For drying air at atmospheric pressure the vapour diffusion coefficient can be calculated as follows [19]:

$$D_v = 3.564 \times 10^{-10}(T_{d,s} + T_g)^{1.75} \quad (17)$$

From Eqs. (10) and (12)–(14) it follows that the droplet specific heat, density and thermal conductivity are all functions of temperature. Therefore, for the set of equations (1)–(17) a numerical solution is preferred [5].

Second drying stage

Heat transfer

The second drying stage begins from the moment when droplet moisture content falls to the critical value and the process of porous crust formation begins on the surface of the droplet. From now, the droplet turns into a wet particle consisting of a dry porous crust surrounding a wet core. The outer diameter of wet particle remains unchangeable, but at the same time the particle wet core shrinks due to evaporation from its surface, and as a result the crust thickness increases. The crust region, whose thermal conductivity is taken as temperature-independent, is considered as a shell of a hollow sphere pierced by a large number of identical straight cylindrical capillaries. By assuming that the wet particle physical properties are isotropic and the coordinate origin is at the centre of the particle, two following equations of energy conservation with corresponding boundary conditions can be written in spherical coordinates [5]:

Crust region of the dried particle:

$$\frac{\partial T_{cr}}{\partial t} = \frac{\alpha_{cr}}{r^2}\frac{\partial}{\partial r}\left(r^2\frac{\partial T_{cr}}{\partial r}\right), R_i(t) \le r \le R_p \quad (18)$$

$$\begin{cases} k_{cr}\frac{\partial T_{cr}}{\partial r} = k_{wc}\frac{\partial T_{wc}}{\partial r} + h_{fg}\frac{\dot{m}_v}{A_i}, & r = R_i(t), \\ T_{wc} = T_{cr}, & r = R_i(t) \\ h(T_g - T_{cr}) = k_{cr}\frac{\partial T_{cr}}{\partial r}, & r = R_p. \end{cases} \quad (19)$$

Wet core region of the dried particle:

$$p_{wc}c_{p,wc}\frac{\partial T_{wc}}{\partial t} = \frac{1}{r^2}\frac{\partial}{\partial r}\left(k_{wc}r^2\frac{\partial T_{wc}}{\partial r}\right),$$

$$0 \le r \le R_i(t) \quad (20)$$

$$\begin{cases} \frac{\partial T_{wc}}{\partial r} = 0, & r = 0, \\ k_{cr}\frac{\partial T_{cr}}{\partial r} = k_{wc}\frac{\partial T_{wc}}{\partial r} = h_{fg}\frac{\dot{m}_v}{A_i}, & r = R_i(t) \\ T_{cr} = T_{wc}, & r = R_i(t), \end{cases} \quad (21)$$

The droplet temperature at the point of critical moisture content is an initial condition for both Eqs. (18) and (20). In the second drying stage the coefficient of heat transfer, *h*, is calculated in the same way as that described above for the first drying stage (Eqs. (3–5)). The only difference is that the emissivity of the particle outer surface ε_r is assumed to be equal to the corresponding value of emissivity of the particle solid fraction, i.e., $\varepsilon_r = \varepsilon_{r,s}$. The receding rate of crust–wet core interface is connected with the rate of liquid evaporation from this interface [15]:

$$\frac{d(R_i)}{dt} = -\frac{1}{\varepsilon\rho_{wc,w}4\pi R_i^2}\dot{m}_v \quad (22)$$

Mass transfer

In order to describe the process of liquid evaporation from the crust–wet core interface inside the wet particle and subsequent vapour flow through the crust pores to the ambient, an isolated capillary pore of the particle crust must be considered. Then, the capillary pore is treated as a straight cylindric body. Therefore, it is convenient to apply the mass, the momentum and the energy conservation laws for the control volume (capillary pore) in cylindrical coordinate system.

Mass conservation

Assuming that within the cylindric crust pore the air–vapour mixture flows isotropically along z-axis only, the equation of mass conservation can be written as follows [20]:

$$\frac{\partial\rho}{\partial t} + \frac{\partial}{\partial z}(\rho v_z) = 0 \quad (23)$$

Momentum conservation

The development of momentum conservation equation brings us to three separate expressions [20]:

r-component:

$$\frac{\partial p}{\partial r} = 0 \Rightarrow p \neq f(r) \quad (24)$$

θ-component:

$$\frac{\partial p}{\partial \theta} = 0 \Rightarrow p \neq f(\theta) \quad (25)$$

z-component:

$$\rho\left(\frac{\partial v_z}{\partial t} + v_z\frac{\partial v_z}{\partial z}\right) = -\frac{\partial p}{\partial z} + \frac{1}{r}\frac{\partial}{\partial r}(r\tau_{rz}) + \frac{1}{r}\frac{\partial\tau_{\theta z}}{\partial\theta} + \frac{\partial\tau_{zz}}{\partial\theta} + pg_z \quad (26)$$

If we assume that only τ_{rz} component of shear stress is nonzero [21] and the gravity term is negligible, it is obtained from Eq. (26):

$$\rho\left(\frac{\partial v_z}{\partial t}+v_z\frac{\partial v_z}{\partial z}\right)=-\frac{\partial p}{\partial z}+\frac{1}{r}\frac{\partial}{\partial r}(r\tau_{rz}) \quad (27)$$

The shear stress at rz-plane is calculated as [20]:

$$\tau_{rz}=\mu\frac{\partial v_z}{\partial r} \quad (28)$$

Substituting Eq. (28) into Eq. (27), we get:

$$\rho\left(\frac{\partial v_z}{\partial t}+v_z\frac{\partial v_z}{\partial z}\right)=-\frac{\partial p}{\partial z}+\frac{\mu}{r}\frac{\partial}{\partial r}\left(r\frac{\partial v_z}{\partial r}\right) \quad (29)$$

Since the crust pore has a small radius, which is in order of microns, it can be expected that the air–vapour flow within the pores will be laminar (Re<2100). Therefore, the viscous forces (right-hand side of Eq. (29)) are much greater than the inertial forces (left-hand side of Eq. (29)). Under such condition, the integration of Eq. (29) brings us to well-known Darcy's law for flow through the porous media [21]:

$$v_z=-\frac{B_k}{\mu}\frac{A_{total}}{A_{pores}}\frac{\partial p}{\partial z}=-\frac{B_k}{\mu\varepsilon^{\beta}}\frac{\partial p}{\partial z} \quad (30)$$

Mass diffusion

By determining the vapour fraction ω_v as

$$\omega_v=\rho_v/\rho \quad (31)$$

and assuming that it changes solely along z-axis of the crust pore, the vapour movement through the crust pores can be described by the following equation of binary diffusion [20]:

$$\rho\left(\frac{\partial \omega_z}{\partial t}+v_z\frac{\partial \omega_v}{\partial z}\right)=\frac{\partial}{\partial z}\left(\rho D_v\frac{\partial \omega_v}{\partial z}\right) \quad (32)$$

The coefficient of vapour diffusion in the air D_v is found from semi-empirical correlation [22]:

$$D_v=2.302\times10^{-5}\frac{p_0}{p}\left(\frac{T}{T_0}\right)^{1.81} \quad (33)$$

where $p_0 = 0.98 \times 10^5$ Pa and $T_0 = 256$K.

Energy conservation

The generalized equation of energy conservation in cylindrical coordinates is [20]:

$$\rho\frac{D_{cp}T}{Dt}+div(-k\nabla T)=\frac{Dp}{Dt}+q'''+\mu\Phi \quad (34)$$

In the considered case, there is no heat source inside the pore, thus $q'''=0$. For gases typically $Pr\cdot Ec<<1$ and so the conduction term div $(-k\nabla T)$ is much greater than viscous dissipation term $\mu\varphi$; therefore, the latter can be neglected in Eq. (34). In the present study we also suppose that due to small length of capillary pore, the changes of air–vapour mixture temperature along the pore are negligible. Consequently, the above temperature is equal to the temperature of the crust–wet core interface. Such an assumption allows us to consider only time dependence of the temperature inside the pores of the particle crust. In addition, the behaviour of air–vapour mixture is considered to be close to ideal gas. As the result of above assumptions, the equation of energy conservation (34) can be reduced to the following [5]:

$$\rho c_p\frac{dT}{dt}=\frac{\partial p}{\partial t}+v_z\frac{\partial p}{\partial z} \quad (35)$$

Constitutive equation

The equation of state for the air–vapour mixture within the capillary pore (by assuming ideal gas) is [5]

$$p=\frac{\rho}{M}\Re T \quad (36)$$

The equation of mass conservation (23) can be rewritten as**:**

$$\frac{d\rho}{dt}+\rho\frac{\partial v_z}{\partial z}=0 \quad (37)$$

Substituting the equation of state (36) into Eq. (37), yields [5]:

$$M\frac{dp}{dt}+p\frac{dM}{dt}-\frac{pM}{T}\frac{dT}{dt}+pM\frac{\partial v_z}{\partial z}=0 \quad (38)$$

Performing the same operation on Eq. (35), it can be got [5]:

$$\frac{dT}{dt}=\frac{\Re T}{Mc_pp}\left(\frac{dp}{dt}+v_z\frac{\partial p}{\partial z}\right) \quad (39)$$

or

$$\frac{dT}{dt}=\frac{\Re T}{Mc_pp}\left(\frac{dp}{dt}\right) \quad (40)$$

Differentiating Eq. (30) by z and neglecting permeability, viscosity and porosity changes along the pore, yields:

$$\frac{\partial v_z}{\partial z}=-\frac{B_k}{\mu\varepsilon^{\beta}}\frac{\partial^2 p}{\partial z^2} \quad (41)$$

Substituting Eqs. (40) and (41) into Eq. (38), it may be obtained [5]:

$$M\frac{dp}{dt}+p\frac{dM}{dt}-\frac{\Re}{c_p}\frac{dp}{dt}-\frac{B_kM}{\mu\varepsilon^{\beta}}p\frac{\partial^2 p}{\partial z^2}=0 \quad (42)$$

For air–vapour mixture it can be shown that

$$M=\frac{M_aM_v}{M_v(1-\omega_v)+\omega_vM_a} \quad (43)$$

and therefore

$$\frac{dM}{dt}=-\frac{M_aM_v(M_a-M_v)}{[M_v(1-\omega_v)+\omega_vM_a]^2}\frac{d\omega_v}{\partial t} \quad (44)$$

$$\frac{dM}{dt}=-\frac{M_a-M_v}{M_aM_v}M^2\frac{d\omega_v}{\partial t} \quad (45)$$

Analogously,

$$\frac{\partial M}{\partial z}=-\frac{M_a-M_v}{M_aM_v}M^2\frac{d\omega_v}{\partial z} \quad (46)$$

Substituting Eq. (45) into Eq. (42), it gets finally:

$$\frac{1}{\gamma p}\frac{dp}{dt}=\frac{M_a-M_v}{M_aM_v}M\frac{d\omega_v}{dt}+\frac{B_kM}{\mu\varepsilon^{\beta}}\frac{\partial^2 p}{\partial z^2} \quad (47)$$

where $\gamma = cp/cv$ is specific heat ratio.

The above equation establishes dependence of both vapour fraction and pressure of air–vapour mixture on time and space coordinates. In order to solve this equation, another relation between *p* and *v*, is needed. For this purpose, the equation of mass diffusion (32) is rewritten as follows [5]:

$$\rho \frac{d\omega_v}{dt} = \frac{\partial}{\partial z}(\rho D_v \frac{\partial \omega_v}{\partial z}) \quad (48)$$

Then, by utilizing the equation of state (36), it may be got:

$$\rho M \frac{d\omega_v}{dt} = \frac{\partial}{\partial z}\left(\rho M\, D_v \frac{\partial \omega_v}{\partial z}\right) \quad (49)$$

Subsequently, differentiation of Eq. (33) gives:

$$\frac{\partial D_v}{\partial z} = 2.302 \times 10^{-5} p_0 \left(\frac{T}{T_0}\right)^{1.81} \left(-\frac{1}{p^2}\right) \frac{\partial p}{\partial z}$$

or

$$\frac{\partial D_v}{\partial z} = -D_v \frac{1}{p} \frac{\partial p}{\partial z} \quad (50)$$

Then, using Eqs. (46) and (50), Eq. (49) can be rewritten as follows [5]:

$$\frac{d\omega_v}{dt} = D_v \left[\frac{\partial^2 \omega_v}{\partial z^2} - \frac{M_a - M_v}{M_a M_v} M \left(\frac{d\omega_v}{\partial z}\right)^2\right] \quad (51)$$

The above equation describes the second relation between p and ω_v. The obtained set of two differential equations (47) and (51), which describe the distribution of pressure and vapour fraction within the pore of particle crust, is the subject for further numerical solution. For this reason, appropriate initial and boundary conditions are developed below [5].

Initial conditions: When a solid crust begins to form, the pressure of air–vapour mixture within an infinitesimal crust pore can be assumed equal to the ambient pressure. The corresponding vapour fraction is calculated as the ratio of partial vapour density to total density of air–vapour mixture over the droplet surface at the end of the first drying stage [5].

Boundary conditions: It should be considered that evaporation of the liquid from the crust–wet core interface is equivalent to inflow of the vapour mass into the pores of the particle crust. The corresponding rate of vapour mass inflow equals the rate of evaporation from the crust–wet core interface [5]:

$$\left(p_v v_{z,v}\right)_{in} A_{pores} = \dot{m}_v \quad (52)$$

Here A_{pores} is the mean area of particle crust cross-section, occupied by pores [8]:

$$A_{pores} = 4\pi \varepsilon^{\beta} R_p R_i \quad (53)$$

The mass balance for the vapour fraction at the boundary z = 0:

$$\left(p_v v_{z,v}\right)_{in} = -\rho D_v \frac{\partial \omega_v}{\partial z} + \omega_v (p v_z)\Big|_{z=0} \quad when\ z = 0 \quad (54)$$

On the other hand, continuity requires:

$$\left(p_v v_{z,v}\right)_{in} = (p v_z)\Big|_{z=0} \quad (55)$$

Substituting Eq. (55) into Eq. (54) gives:

$$-\rho D_v \frac{\partial \omega_v}{\partial z} = (1 - \omega_v)(p v_z)_{z=0}, when\ z = 0 \quad (56)$$

By substituting Eq. (52), the above equation can be rewritten as

$$-\rho D_v \frac{\partial \omega_v}{\partial z} = (1 - \omega_v) \frac{m_v}{A_{pores}} \quad when\ z = 0 \quad (57)$$

Finally, substituting Eqs. (22) and (53) into Eq. (57), gives:

$$-\rho D_v \frac{\partial \omega_v}{\partial z} = (1 - \omega_v)\varepsilon^{1-\beta} \rho_{wc,w} \frac{R_i}{R_p} \frac{d(R_i)}{dt} \quad when\ z = 0 \quad (58)$$

It may be assumed that the liquid fraction in the particle wet core is in equilibrium with the vapour over the crust–wet core interface, i.e., [5]:

$$\omega_v = \frac{\rho_{v,sat}(T_{wc,s})}{\rho} \quad when\ \ z = 0 \quad (59)$$

Then, the pressure of air–vapour mixture at the crust–wet core interface can be found by combining the above equation with the ideal gas law (36):

$$p = p_{v,sat}(T_{wc,s}) \frac{M_v}{\omega v M} \quad when\ z = 0 \quad (60)$$

For the second boundary of the capillary pore ($z = L_p$), the following equation of mass conservation for vapour fraction can be developed:

$$\left[-\rho D_v \frac{\partial \omega_v}{\partial z} + \omega_v (p v_z)\right] A_{pores} = p h_D (\omega_v - \omega_{v,\infty}) A_p \quad when\ z = L_p$$

or

$$-\rho D_v \frac{\partial \omega_v}{\partial z} + \omega_v (p v_z) = p h_D (\omega_v - \omega_{v,\infty}) \frac{R_p}{R_i} \varepsilon^{-\beta} \quad when\ z = L_p \quad (61)$$

it may be assumed that the pressure at the particle outer surface is equal to the drying air pressure. Therefore, for $z = Lp$ [5]:

$$p\,\big|_{z=L_p} = p_g \quad (62)$$

Combining the above condition with the equation of state (36) and substituting the result into Eq. (61), yields to:

$$-D_v \frac{\partial \omega_v}{\partial z} + \omega_v (pv_z) \frac{\Re T_{wc,s}}{p_g M} = h_D \left(\omega_v - \omega_{v,\infty}\right) \frac{R_p}{R_i} \varepsilon^{-\beta} \quad when\ z = L_p \tag{63}$$

In such a way, the pressure of air–vapour mixture and the vapour fraction within the capillary pores of the particle crust is determined by the set of differential equations (47) and (51), and their boundary conditions (58), (60), (62) and (63) [5].

SIMULATION IMPLEMENTATION STAGES

In the current research named modeling the silica particles drying and dehumidifying process, different equations such as mass transfer, heat transfer etc. are numerically analyzed. As figure 2 shows, this process includes two different stages. First stage is introduced as the drying stage; in this stage: the droplets surrounding the particles are evaporated from the solid surface and crust by the use of heating; but it is in the second stage where the drying process is conducted completely from the wet particle surface. Thus, according to hypotheses, the equations are written down for each stage and based on some simplifying hypotheses which are mentioned below, the problem is numerically analyzed.

First drying stage

With regard to what can be perceived from the physics of the problem, the hypothesis of compact thermal capacity does not provide acceptable results for thermal analysis of this part; thus assuming that particle is spherical, its properties are isotropic and that temperature changes are only in direction of radius of the particle, the energy equation of the particle which is in fact related to its surrounding water is stated as 1-17 equations. Now for analyzing the above mentioned equation in a discrete form and for using it in numerical analysis, firstly it is necessary to extract the required properties from the related equations. For example, in the above mentioned convection boundary condition, both effect of radiation heat transfer and convection are considered and for convective heat transfer coefficient, the relation 4 is suggested. It must be noted that coding for equations such as the above mentioned equation is very simple and that is exactly the reason why they are provided in the program. Thus for further explanations in this regard, the best solution is referring to the code.

Second drying stage

The procedures in the second stage are the same as what has been explained in the first stage with this difference that the second stage itself consists of two areas including dried particle crust and its wet core and the energy equations of each one and boundary conditions are provided as 18-21 relations. Thus the discrete form of energy equation is the same as first stage with this difference that some of its independent parameters are separately calculated. For example, one of these parameters is the silica particle thermal diffusivity and the same as first stage, this relation was also determined clearly by the use of finite difference method and coding. By applying the same method for the second stage energy equation, and regarding what has been achieved in the first stage, a passive matrix of temperature and a product-matrix of its coefficients are provided that must be solved simultaneously for our mentioned problem. It is possible to use different methods such as LU method for solving this matrix. It must be noted that due to high volume of equations and number of considered points and nodes for the numerical analysis of the problem, since the problem is explicitly coded, thus there is always a stabilizer (for reaching the answer) based on the number of time and place nodes. On the other hand, since by the increasing number of equations, the program may encounter problems in the so-called blind loops and the problem-solving becomes divergent, thus in addition to determining the convergence of the problem, and that this amount must be an optimal amount for fast problem-solving, at the end, the number of time and space nodes are selected. It is clear that the more the number of nodes provided the observance of convergence condition, the more accurate the answers; thus as the output results of the above mentioned program show, this optimal value is chosen relatively well. It is possible to use MATLAB software for solving the final matrix through LU method; because this software has an appropriate code for solving this problem; but for a better understanding of this problem these relations are brought separately in the code as algebraic equations of 2 to 6 (regarding the 5 diagonal matrix formed) and by solving them we can finally reach the desirable results.

RESULTS & DISCUSSION

In this part the simulation results by the use of MATLAB software are provided. By the use of numerical solution of developed model, the

simulation of dehumidifying a droplet including silica particles is conducted. No specific connective material has been used. Liquid and solid fractions emissions of the droplet are considered as the constant amounts and they are 0.96 and 0.8, respectively. During the studies, different parameters are changed: dehumidifier temperature is changed in the range of 150-750°C; dehumidifier speed is between 2.5 to 3.5 meter per second and diagonal of stem droplet is between 0.25 to 2 millimeters and porous shell particle is changed in the distance of 0.1 and 0.4. Important properties of the wet particle are surveyed during the simulation: the outer surface and center of droplets temperature, droplet moisture and mass, vapor and vapor-air pressure fraction in the middle surface of core of the wet shell inside the particle pores. A number of computational results of the developed model for different dehumidifier temperatures are shown in figures 3 to 6. In these simulations, below amounts are used for dehumidifying parameters: droplet initial temperature of 19°C, droplet initial diagonal of 2 millimeters, porous shell particle, final wet content 0.05 and dehumidifier speed of 1.14 meter per second.

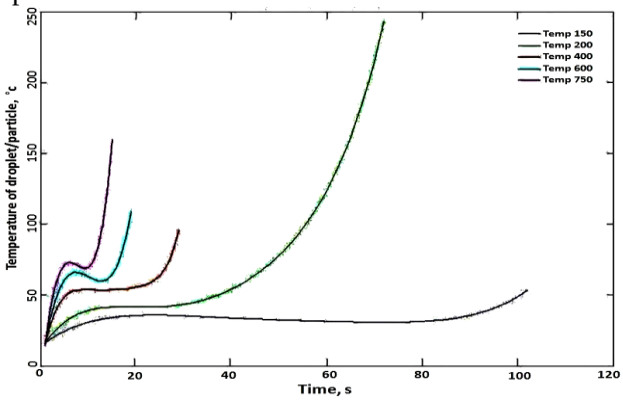

Fig. 3. Temperature changes according to time at different air temperatures.

The initial temperature of silica droplet is 19°C; at the initial dehumidifying stage we have increased temperature; by increasing the temperature the droplet reaches a special heat and evaporation of the droplet surface starts; in a relatively fixed interval the evaporation of droplet surface is conducted. When the liquid amount within the droplet reaches a critical amount, a very thin layer of solid dry shell is formed in the outer surface of the droplet; from this point, the second level of dehumidifying begins. As it is observable in figure 3, there is increased temperature as the second stage begins. The more the temperature increases, the less time is needed and the faster the dehumidifying process is conducted. In the figure 4, the maximum amount of mass is at the beginning of dehumidifying and then gradually over time, the droplet mass decreases. Figure 5 is the diagram of moisture according to time; the highest amount of moisture is at the beginning of dehumidifying and then gradually over time, the moisture decreases.

In figures 6 and 7 the gradual increase of pressure and vapor fraction in the middle surface of shell and wet core are observable. Increased particle temperature results in surface evaporation of the liquid fraction in the wet core of the particle and as a result, vapor fraction and partial pressure of vapor in the middle surface of wet core shell are increased.

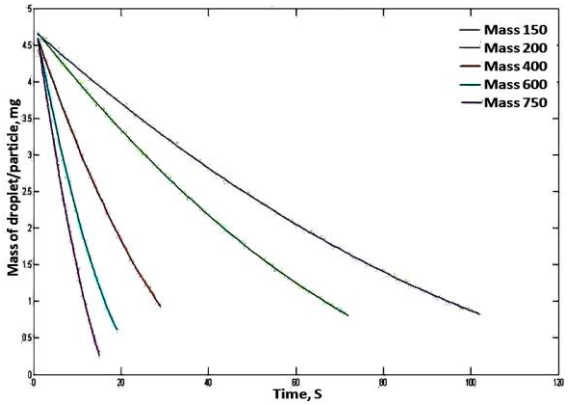

Fig. 4. Mass changes according to time at different temperatures.

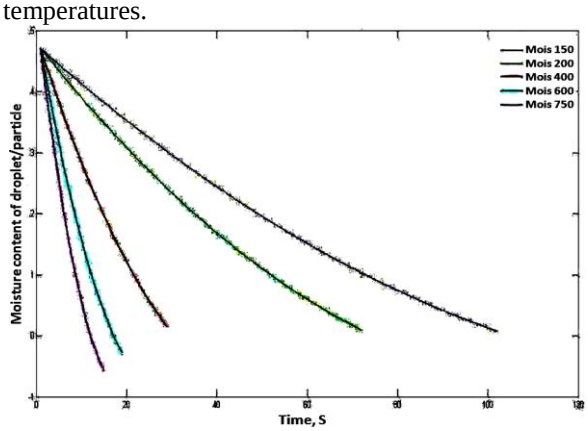

Fig. 5. Moisture changes according to time at different temperatures.

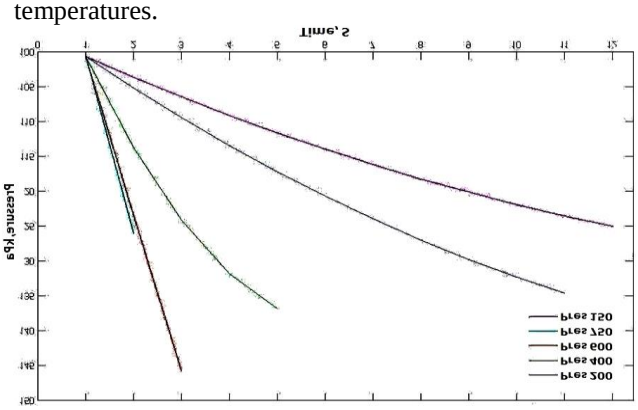

Fig. 6. Pressure distribution in the middle surface of wet core shell during the second stage of dehumidifying.

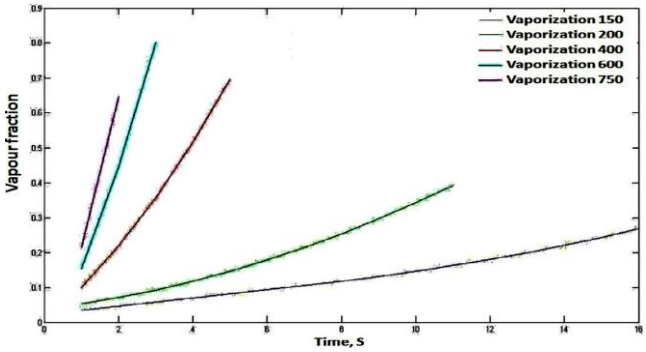

Fig. 7. Vapour fraction distribution in the middle surface of wet core shell during the second stage of dehumidifying.

In other words, partial pressure of dry air above the middle surface gradually decreases during the dehumidifying as a result of dry air release from the dehumidifier in the pores toward the wet core of particle and forced air-vapor stream in the opposite direction. Imbalance between these two processes results in increased vapor fraction pressure and decreased dry air pressure as a result of creation of air-vapor pressure in the middle surface of wet core and shell; and also the amount of vapor fraction increases. As a result, it is concluded that in the studied samples, mechanism of release of vapor has a more important role compared to the forced vapor flow caused by pressure difference in the porous shell particle.

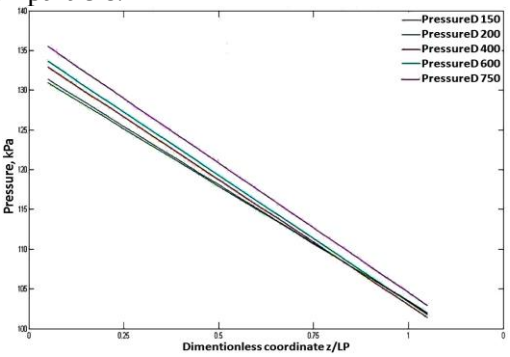

Fig. 8. Pressure distribution changes in the shell pores.

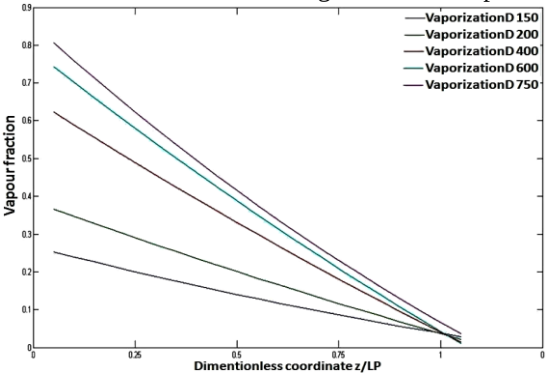

Fig. 9. Vapor fraction distribution changes in shell pores.

In the figures 8 and 9, vapor fraction and pressure from particle core in the shell pores toward the outer surface decrease linearly.

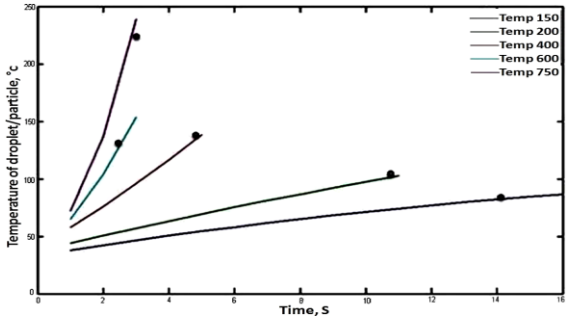

Fig. 10. Particle surface temperature changes according to time in second drying stage.

In the second drying stage under different temperatures (as it is observable in the figure-10) the particle surface temperature increases over time.

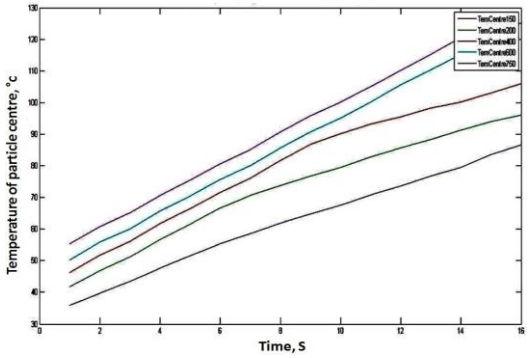

Fig. 11. Particle center temperature changes according to time in second drying stage.

Figure 11 shows that in second drying stage under different temperatures, the particle center temperature increases over time.

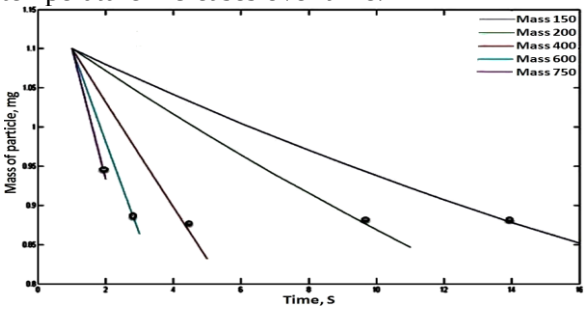

Fig. 12. Particle mass changes according to time in the second drying stage.

According to figure 12, it may be said that in the second drying stage under different temperatures, the particle mass gradually decreased over time.

CONCLUSION

In this study, it has been tried to take a step forward in the development of simulation of drying materials by the use of MATLAB software. Thus, a theoretical model of heat and mass transfer for dehumidifying the wet particle was investigated.

The surveyed sample includes the completely unstable properties of heat and mass in the second dehumidifying stage and it makes the calculation of vapor fraction and air-vapor pressure inside narrow pores of the shell particle possible. The model equations were solved numerically and the dehumidifying simulation is conducted. The research important result is the continuous increase of particle pressure in the middle surface of wet core shell. The process of mass transfer in the second dehumidifying stage is described by the use of hypotheses of semi steady-state and linear pressure profile in shell pores. It is pertinent to put on record which this model needs less computer time for calculations and this provides the use of this model with reasonable accuracy for samples requiring use of fast calculations.

Acknowledgment. *This scientific product was extracted through a research project implemented from funding of research projects of Yasooj Branch, Islamic Azad University*.

NOTATION

A surface area, m^2
A_{pores} mean area of crust cross-section, occupied by pores, m^2
A_{total} total mean area of crust cross-section, m^2
b empirical coefficient
B Spalding number
B_i Biot number
B_k crust permeability, m^2
c mass concentration of solid fraction, kg kg^{-1}
c_p specific heat under constant pressure, J kg^{-1} K^{-1}
c_v specific heat under constant volume, J kg^{-1} K^{-1}
d diameter, m
D_v coefficient of vapour diffusion, m^2 s^{-1}
E_c Eckert number
F_o Fourier number
g acceleration of gravity, ms^{-2}
h heat transfer coefficient, Wm^{-2} K^{-1}
h_c coefficient of convection heat transfer, Wm^{-2} K^{-1}
h_D mass transfer coefficient, ms^{-1}
h_{fg} specific heat of evaporation, J kg^{-1}
h_r coefficient of radiation heat transfer, Wm^{-2} K^{-1}
k thermal conductivity, Wm^{-1} K^{-1}
L_p length of crust pore, m
m mass, kg
M molecular weight, kg mol^{-1}
$\dot{m}_v$ rate of evaporation, kg s^{-1}
n empirical coefficient
Nu Nusselt number
p pressure, Pa
p_0 reference pressure, Pa
P_r Prandtl number
q_t specific heat of mixing, J kg^{-1}
q^n heat source term, Wm^{-3}
r radial coordinate, m
R radius, m
$\Re$ universal gas constant, J mol^{-1} K^{-1}
Re Reynolds number
s space coordinate, m
Sc Schmidt number
Sh Sherwood number
t time, s
T temperature, K
T_0 reference temperature, K
u_g velocity of drying agent, ms^{-1}
V volume, m^3
X moisture content (dry basis), kg kg^{-1}
z axial coordinate, m

Greek letters

α thermal diffusivity, m^2 s^{-1}
α_m empirical coefficient
α_T coefficient of thermal expansion, K^{-1}
β empirical power coefficient
γ specific heat ratio
δ droplet void fraction
ε crust porosity
ε_r emissivity
θ angular coordinate
μ dynamic viscosity, kgm^{-1} s^{-1}
ρ density, kgm^{-3}
σ Stefan–Boltzmann constant, Wm^{-2} K^{-4}
τ shear stress, Pa
υ velocity, ms^{-1}
φ dissipation term, J kg^{-1} m^{-2}
ω_v vapour fraction

Subscripts

a air, dry air fraction
atm atmospheric
c crust capillary
cr particle crust
d droplet
f final point of drying process
flow forced flow
g drying agent
i crust–wet core interface
in inflow
m air–vapour mixture
out outflow
p particle
pores crust pores

r	radial direction
s	solid fraction or surface
sat	saturated
v	vapour, vapour fraction
w	water
wc	particle wet core
z	axial direction
0	initial point of drying process
∞	bulk of drying agent
Θ	tangential direction

REFERENCES

1 .K.A. Haghi, D. Rondot, *Iran. J. Chem. & Chem. Eng.*, **23**, 25-34 (2004).
2. A.K. Haghi, *J. Comp. Appl. Mech.*, **2**, 195 (2001).
3. A.K. Haghi, *J. Theor. Appl. Mech.*, **32**,. 47 (2002).
4. A.K. Haghi, *Int. J. Appl. Mech. Eng.*, **8**, 233 (2003).
5. M. Mezhericher, A. Levy, I. Borde, *Chem. Eng. Sci*., **63,**. 12 (2008).
6. H. Mortezapour, B., Ghobadian, M.H. Khoshtaghaza, S. Minaei, *J. Agr. Sci. Tech*., **16**, 33 (2014).
7. M. Mezhericher, A. Levy, I. Borde, *Drying Technol*., **25**, 1025 (2007a).
8. M. Mezhericher, A. Levy, I. Borde, *Chem. Eng. Process*, **47**, 1404 (2007b.).
9. May be found in: www.tecoma.it, (2014).
10. D. Nesip, O.O. Hilmi, N.E. Ahmet, U. Yusuf, *Drying Technol.*, **25,** 391 (2007).
11. M.M. Farid, *Chem. Eng. Sci.*, **58**, 2985 (2003).
12. H.W. Cheong, G.V. Jeffreys, C.J. Mumford, *AIChE. J.*, **32**, 1334 (1986).
13. Chen, X. D., Xie,G. Z., *Trans. Ins. Ch.E., Part C*, **75**, 213 (1997).
14. N. Abuaf., F.W. Staub, (Edrs), Drying '86, Vol. 1, Hemisphere, Washington, DC, pp. 277–284 (1986).
15. D. Levi-Hevroni, A. Levy, I. Borde, *Drying Technol.*, **13**, 1187 (1995).
16. J.P. Holman, Heat Transfer. McGraw-Hill, New York (2002).
17. V.A. Kirillin, A.E. Sheindlin, Thermodynamics of Solutions, Moscow, (1956).
18. Chen, X.D., Peng, X.F., *Drying Technol.*, **23**, 83 (2005).
19. V.A. Grigoriev, V.M. Zorin, Thermal Engineering Handbook, Part 1, Moscow, (1988).
20. L.C. Burmeister, J. Wiley, New York (1983).
21. R.E. Cunningham, R.J.J. Williams, Plenum Press, New York (1980).
22.E.R.G. Eckert, R.M.H. Drake, McGraw-Hill, New York, (1972).